ELSEVIER

Journal of Chromatography A, 871 (2000) 449–460

JOURNAL OF CHROMATOGRAPHY A

www.elsevier.com/locate/chroma

Continuous split-flow thin cell and gravitational field-flow fractionation of wheat starch particles

Catia Contado[a,*], Pierluigi Reschiglian[b], Stefania Faccini[a], Andrea Zattoni[b], Francesco Dondi[a]

[a]*Department of Chemistry, University of Ferrara, Via L. Borsari 46, I-44100 Ferrara, Italy*
[b]*Department of Chemistry "G.Ciamician", University of Bologna, Via Selmi 2, I-40126 Bologna, Italy*

Received 31 May 1999; received in revised form 5 November 1999; accepted 11 November 1999

Abstract

The combined employment of the SPLITT (split-flow thin) cell — a relatively new system for fast, continuous binary separation — and of gravitational field-flow fractionation (GrFFF) — a fractionation technique suitable for micron particle size distribution determination — was investigated for starch separation and characterization. Emphasis is placed on the main advantages of both techniques: operating under gentle earth gravity field, low cost and ease of maintenance. The reproducibility of GrFFF is demonstrated. Both the SPLITT separation and GrFFF fractionation results were checked by optical microscopy. Application examples of typical starch fractionation experiments are reported and discussed.

Keywords: Split-flow thin cell fractionation; Field-flow fractionation; Particle size distribution; Wheat; Starch

1. Introduction

Starch is an important raw material for industrial applications, both for food and nonfood purposes, and the market for these products is expanding [1]. In its native granular form, starch has few uses. To release the polymer properties, granule disruption, hydrolysis and, sometimes, modification are also necessary. These can be achieved through chemical and/or physical processes [1].

Granules range from 1 to 55 μm in diameter and, depending on the kind of starch, they may have a regular rounded shape. Some starch samples show a characteristic bimodal granule population (called respectively A and B) (e.g. barley, wheat, rye), while others (e.g. rice) have a monomodal particle size distribution (PSD). Some modification processes of industrial interest are size dependent, as, for example, the enzyme hydrolytic action that takes place during the brewery malting process and which is more efficient on large barley granules (population A). The relatively high density of starch granules (1.5 g/cm^3) facilitates separation by centrifugation/gravity sedimentation or by filtration during isolation, chemical modifications and washing [2], especially for the largest dimensions. Unfortunately these procedures prove quite time-consuming when a suitable amount of product must be handled for further analytical characterization.

In response to industrial demand for fast size separation and rapid determination of granule PSD,

*Corresponding author.
E-mail address: kat@dns.unife.it (C. Contado)

0021-9673/00/$ – see front matter
PII: S0021-9673(99)01191-7

the present work considers, for the first time, the complementary employment of two separation techniques specifically suited to particles separation and characterization: the split-flow thin cell (SPLITT) and gravitational field-flow fractionation (GrFFF), a field-flow fractionation (FFF) subtechnique. The advantage of this joint use lies in the fact that the first technique (SPLITT) is a large scale, binary separation method suitable for either bimodal or broadly dispersed samples, whereas the second (GrFFF) is an analytical scale fractionation, chromatography-like technique that is most suitable for PSD analysis of moderately dispersed, micron-size samples.

A SPLITT fractionation system employing gravitational force is illustrated in Fig. 1a. The use of a SPLITT fractionation system has proved advantageous for many analytical [3–5] and preparative [6,7] applications because it is fast, simple, theoretically tractable, providing high resolution and gentle, continuous processing within a relatively inexpensive environment. The SPLITT cell has already proved to be a continuous, fast and tunable preparatory tool for the separation of different dimensional fractions of a wheat starch sample [8,9]. On the other hand, accurate PSD of the SPLITT fractions is an unavoidable task for both the SPLITT optimization procedure and for the final evaluation of the preparative fractionation results.

In general FFF has proved to be a rapid method

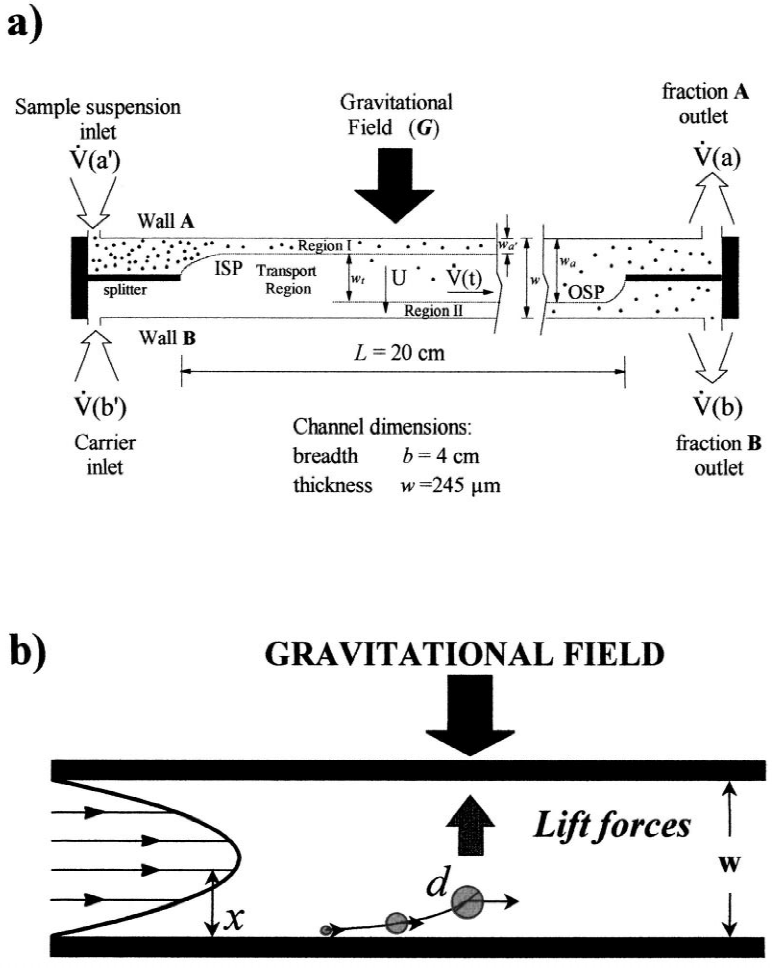

Fig. 1. Channel cross-sections. (a) SPLITT cell; (b) GrFFF.

for the determination of PSD and/or particle attributes such as the mean diameter and polydispersity of particulate samples [10]. Among FFF procedures, the one most frequently used for the dimensional characterization of particulate systems of micron-size range is the centrifugal sedimentation field-flow fractionation (SdFFF) in the steric elution mode. For PSD purposes, this technique has been successfully applied using the density compensation procedure [8,11,12]. GrFFF is a subset of SdFFF which has already been proven able to fractionate starch granules on an analytical scale [13]. A scheme of the GrFFF fractionation mechanism is reported in Fig. 1b. The great advantage of GrFFF as compared to other FFF techniques lies in its very low cost and easy implementation in a standard HPLC system (the channel can simply replace the column). This simplicity and economics make it possible for laboratories not specialized in PSD analysis to perform dimensional characterization of supermicron particle dispersions relatively easily and inexpensively [14,15]. Specifically, with respect to the centrifugal SdFFF, GrFFF has another practical advantage: like SPLITT, GrFFF operates under a weak gravitational field (earth gravity field) high enough to fractionate particles within the density and dimensional range of starch granules, as previously indicated. On the other hand, the earth gravity field is also weak enough to guarantee gentle fractionation processes for delicate samples such as starch granules. Moreover, elution in both SPLITT and GrFFF channels can be continuously monitored during separation, and channel walls can easily be cleaned whenever required.

Optical microscopy (OM) was used to both test the goodness of the performed SPLITT separations and to convert the time axis of the GrFFF fractograms to size. Although other sizing techniques for PSD analysis of micron-size particles based on laser scattering (as flow cytometry) or electrical properties (as the Coulter counter principle) are also accurate and less time-consuming, OM may be preferred since it is an ''absolute'' method of sizing, based on direct optic observations of the sample. In the first case the percentages of the granules found above and below the cut-off diameter and their dimensions have been computed; in the second case some collected GrFFF fractions were photographed and the granules measured.

Since the main goal of this work was to study the effectiveness of the SPLITT–GrFFF synergism, the whole starch sample employed here (with a broad 1–50 μm size range) was pretreated to obtain a sample (1–15 μm) suitable for SPLITT cell separation. In fact, when broad size distribution samples are SPLITT separated, it is best to clean the sample of oversized granules, i.e., those more than twice the cut-off diameter set for the SPLITT separation. For this reason, the commercial sample was previously cut at around 15 μm by applying the classical sedimentation procedure [16]. The same result would have been obtained by using the SPLITT cell also for such a preliminary cut.

2. Theory

Fig. 1a shows the principles underlying the operation of a simple binary SPLITT cell. The theory defining the SPLITT separation has been described in numerous publications [Refs. 6,17 and therein]. Due to the action of the external field, particles are transported differentially across the thickness w of the cell. Rapidly migrating particles are separated from those undergoing slower transport by means of an outlet splitter that divides the channel laminae into two outlet substreams, **a** and **b**.

The effectiveness of the SPLITT process is enhanced by actively controlling the positions of the inlet splitting plane (ISP) and the outlet splitting plane: such control is achieved by varying the flow-rates of inlet ($\dot{V}(a')$ and $\dot{V}(b')$) and outlet ($\dot{V}(a)$ and $\dot{V}(b)$) substreams.

It is assumed that particles, introduced as a suspension through inlet **a**′, are driven at constant velocity U from wall A to wall B during their residence in the SPLITT cell. As a consequence of this uniform transport, the particles are driven across a thin filament (transport region t_r) of the flowing liquid. The volumetric flow-rate $\Delta\dot{V}$ of the lamina traversed by a compact spherical particle is simply given by [17]:

$$\Delta\dot{V} = bLU = \frac{bLGd^2|\Delta\rho|}{18\eta} \quad (1)$$

containing the physical dimensions of the channel: b

is the width and L the length. The sedimentation velocity of the particle U can be made explicit in terms of the acceleration of gravity G, the particle diameter d, the difference $\Delta\rho$ between particle density ρ_p and carrier density ρ_l and the viscosity of the carrier η. $\Delta\dot{V}$ must thus be interpreted as a hypothetical volumetric flow-rate, connected to the sedimentation velocity U.

The total volumetric flow-rate $\dot{V}$ in the channel can be written in several equivalent forms, for example, as the sum of the flow-rates of constituent laminae [18]:

$$\dot{V} = \dot{V}(a') + \dot{V}(b') = \dot{V}(a) + \dot{V}(b) = \dot{V}(a') + \dot{V}(t) + \dot{V}(b) \quad (2)$$

where $\dot{V}(t)$ is the fluid flow proceeding in the transport layer. This flow-rate can be obtained from Eq. (2) as:

$$\dot{V}(t) = \dot{V}(a) - \dot{V}(a') = \dot{V}(b') - \dot{V}(b) \quad (3)$$

Of critical importance are the relative values of $\Delta\dot{V}$ and $\dot{V}(t)$, indicating whether particles exit the channel through outlet **a** or **b**. For a sample introduced close to the ISP, particles exit from outlet **a** if:

$$\Delta\dot{V} \leq \dot{V}(t) \quad (4)$$

and from outlet **b** if:

$$\Delta\dot{V} > \dot{V}(t) \quad (5)$$

The diameter at which 50% of the particles exit outlet **b** is called the cut-off diameter d_c, expressed as [19,20]:

$$d_c = \sqrt{\frac{18\eta(\dot{V}(a) - 0.5\dot{V}(a'))}{bL|\Delta\rho|G}} \quad (6)$$

This equation has been chosen because it is based on the particle model which better describes the real sample here considered [17]. Once d_c has been chosen for a given channel, the difference between $\dot{V}(a)$ and $0.5\dot{V}(a')$ is set according to Eq. (6).

FFF retention theory has been fully explained elsewhere (Ref. [10] and references therein). Since in GrFFF, retention may be affected by either hydrodynamic forces able to lift particles away from the wall (see scheme in Fig. 1b) [21] or by other effects such as those linked to the composition of the mobile phase and channel walls [22,23], size determination of sample cuts fractionated by SPLITT can be obtained through GrFFF by means of a calibration plot that can be worked out through the expression of the fractionation selectivity [11,24]

$$\log V_{r,i} = -S_d \log d_i + \log V_{r,1} \quad (7)$$

$$S_d = -\frac{\delta \log V_{r,i}}{\delta \log d_i} \quad (8)$$

where $V_{r,1}$ is the retention volume of a particle of unit diameter. Once selectivity is determined from the slope of the linear regression $\log V_{r,i}$ vs. $\log d_i$, in the selected dimensional range the conversion from retention ratio to size can be performed for any data point of the fractogram by rearranging Eq. (8) to obtain

$$d_i = \left(\frac{V_{r,i}}{V_{r,1}}\right)^{-\frac{1}{S_d}} \quad (9)$$

Sizing based on Eqs. (7)–(9) does not take into account the density distribution of the sample. In fact, it was reported for sizing in flow FFF and SdFFF for which, respectively, retention does not depend on density [24] or it is density-compensated [11]. However, if the calibration plot [Eq. (7)] is performed on eluted samples and an independent method of sizing such as OM is used, density variations of the sample itself are compensated and the method can be applied also to GrFFF.

3. Experimental

For all the SPLITT–GrFFF experiments, starch from wheat samples (Catalog Number 85649, Fluka, Buchs, Switzerland), with a measured, mean granule density of 1.54 g/ml, was employed. The fraction **S1** (1–15 μm) of the total sample (1–50 μm) has been separated through the SPLITT cell as a suspension dispersed in Milli-Q water (Millipore, Bedford, MA, USA) with 0.05% (v/v) of Triton X-100 (see Table 1 for the experimental details and Fig. 2 for separation scheme).

The SPLITT cell used in this study, assembled as previously reported [17] is shown in Fig. 1a. Three

Table 1
Experimental SPLITT separation conditions; theoretical diameter cut-off $d_c = 10$ μm, $\Delta\dot{V} \sim 14$ ml/min, $w = 245$ μm

$\dot{V}(a')$ (ml/min)	$\dot{V}(b')$ (ml/min)	$\dot{V}(a)$ (ml/min)	$\dot{V}(b)$ (ml/min)	$\dot{V}$ (ml/min)	$\dot{V}(a')/\dot{V}(t)$	$\dot{V}(b')/\dot{V}(t)$	$w_{a'}$ (μm)	w_t (μm)
5	15.5	19.0	1.5	20.5	0.24	0.75	204	126

peristaltic pumps, a Minitan [Millipore, Vimodrone (Mi), Italy] and two Minipuls3 (Gilson, Middleton, WI, USA) were employed to provide independent flow streams to inlets **a**′, **b**′ and to regulate the outlet flow-rate **a**. The fourth flow-rate at outlet **b** was thus automatically regulated. The SPLITT cell was used in the so-called transport mode, where the diffusion mechanisms are not relevant [8,9,17]. The experimental conditions used for the separation are summarized in Table 1.

The GrFFF channel was built up as described elsewhere [14,15]: two mirror-polished glass plates were clamped together over a Mylar sheet from which the channel volume had been removed. The ribbon-like channel was 0.0132 cm thick, 2 cm wide and 30 cm long tip-to-tip. The flow-rate was set at 2 ml/min. The void volume was determined at 0.802 ml with an unretained probe (K_2CrO_4). The channel replaced the column of a standard HPLC system: the carrier flow was generated by a Model 2510 HPLC

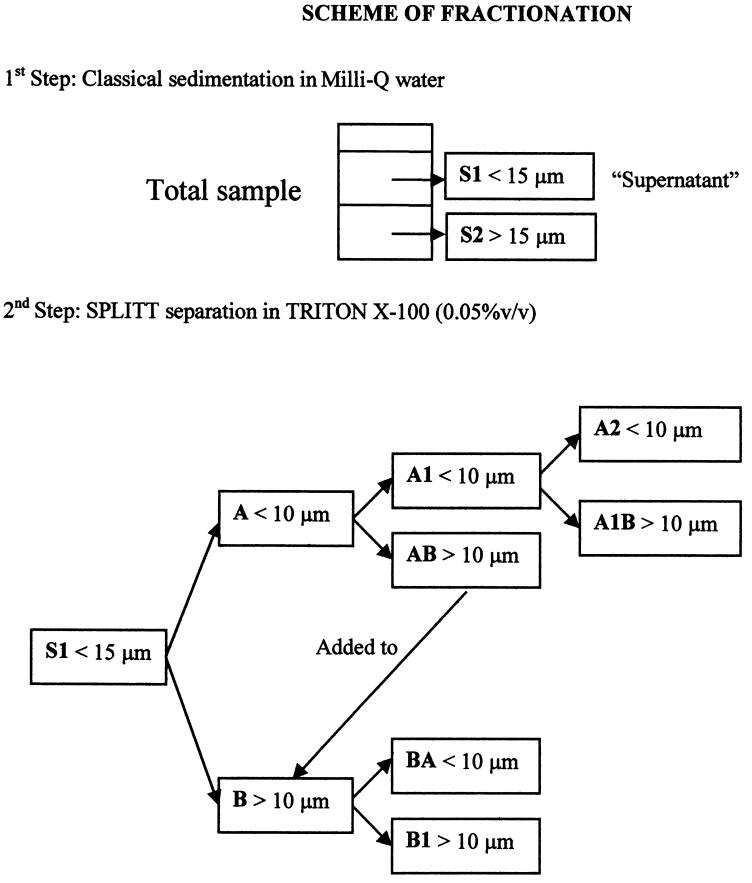

Fig. 2. SPLITT fractionation scheme.

pump and the channel outlet was connected to a Model 2550 UV detector (Varian, Walnut Creek, CA, USA) operating at 330 nm. The signal was recorded on a strip-chart integrator Model Mega 2 (Carlo Erba, Milan, Italy). Fractograms were digitized using a flat-bed scanner and an ASCII file obtained by vectorizing the scanned bitmap by using Un-Scan It (Silk Scientific, Orem, UT, USA).

The total sample and the dry fractions coming from SPLITT separations were prepared as 1% (w/v) suspensions in Milli-Q water, added with 0.05% (w/v) sodium dodecyl sulfate (SDS) and 0.01% (w/v) NaN_3, if necessary. The volumes injected in the GrFFF channel were always 10 μl. The eluent was a 0.05% (w/v) SDS, 0.01% (w/v) NaN_3 solution in Milli-Q water. Sample fractions from SPLITT were allowed to equilibrate at least 10 h in the dispersing medium after the preparation of the dispersion, and sonicated 2 min before GrFFF runs. Fig. 3 reports seven GrFFF fractograms of one of the SPLITT fractions (fraction **A2,** see the Section 3.1), each recorded at a different equilibration time. An increase in separation with an increase in equilibration time is evident. This finding can be due to particle swelling after being dispersed in the aqueous medium and to the reduction in particle aggregation.

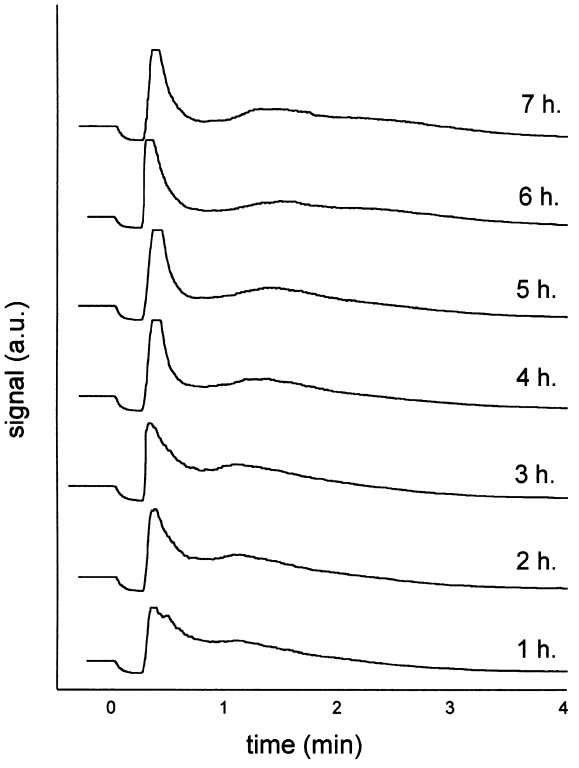

Fig. 3. Dependence of the GrFFF separation profile on sample equilibration time — SPLITT fraction **A2** (see Fig. 2).

Narrow GrFFF fractions of eluted starch were manually collected in centrifuge tubes, left to settle for 18 h at 4°C and eventually examined by an optical microscope after iodine staining. In order to assess the random character of the OM fields choice, which influences accuracy of OM sizing, OM pictures where independently taken in two different laboratories. Subsequently, all printed pictures were digitalized through a high-resolution flat-bed scanner. Size measures on the electronic versions of all OM pictures were performed in Corel PhotoPaint 8.0 (Corel, Ottawa, Canada) once a proper conversion was determined (20 μm = 38 dots per linear inch) to set a meshing grid superimposed to the images. By this way, all the photographed particles were measured by means of two readings for each particle: one along the horizontal and one along the vertical axis. Finally, all the readings were averaged and relevant standard deviations calculated. A tenfold accumulation of GrFFF fractions was necessary to collect an adequate number of particles for OM measurements.

3.1. SPLITT separation: experimental design

In order to prepare the starch sample for the SPLITT separation, a preliminary cut was performed applying the classical sedimentation procedure previously described [16]. The cut-off diameter was set at 15 μm in order to remove most of the oversized granules, — i.e., those particles with a diameter more than double the cut-off diameter set for the SPLITT separation — from the broad size distribution. This was also necessary because of the high ratio between biggest and smallest granules in the total sample. Six g of starch were washed 20 times with Milli-Q water: the 20 fractions, containing the lightest granules, were pooled into a single fraction labeled **S1**, whereas the fraction containing granules larger than 15 μm, **S2,** was collected from the bottom of the sedimentation vessel. Fraction **S1** (<15 μm) was filtered by using hydrophilic MF Millipore mem-

brane filters, 1.2 μm pore dimensions, and the granules were air-dried. Fraction **S2** was dried by replacing the Milli-Q water on which they were dispersed with ethanol and by placing the wet granules in an oven at 45°C for 24 h.

The dried fraction **S1** (<15 μm) was dispersed in a solution of Triton X-100 (0.05%, v/v) in order to obtain a ~0.4% (w/v) suspension to be separated by the SPLITT cell following the scheme reported in Fig. 2. The same solution composition was used for the auxiliary carrier flowing into the SPLITT cell through inlet **b′**. For specific application purposes, the SPLITT cut-off diameter was intentionally set at 10 μm, since this separation strategy can also be applied to fractionate and isolate barley granules, whose PSD is known to be bimodal [13]. It has actually been demonstrated that, in the brewery, the barley granule fraction above 10 μm are better digested during the malting process, thus giving a higher alcoholic yield [13].

As a consequence of the chosen fractionation strategy, this first cut produced two fractions, **A** and **B**, respectively containing particles with nominal dimensions above and below 10 μm. Fraction **A** — containing particles with nominal dimensions lower than 10 μm — underwent two further separations always using the same dimensional cut-off. The second cut produced the fraction **A1**, still containing particles with nominal dimension lower than 10 μm, and a fraction **AB**, containing particles in the 10–15 μm range. This last fraction was added to fraction **B** and further separated to give the final fraction **B1** (>10 μm), and a fraction **BA**, containing granules <10 μm. The fraction **A1** was cleaned again and yielded the final fraction **A2**, containing only granules smaller than 10 μm, and a fraction **A1B**, containing granules larger than 10 μm.

At the end of this treatment the fraction **A2** (<10 μm) was filtered and air-dried, and the fraction **B1** ($10<d_c<15$ μm) was dried by substituting the Milli-Q water with ethanol. These two fractions were eventually fractionated on analytical scale by GrFFF in order to determine their PSD.

4. Discussion

In this first work on SPLITT–GrFFF separation and characterization of starch granules, previously optimized SPLITT operating conditions (i.e. the effect of carrier composition, relative flow-rates) were applied [8]. Fig. 4 reports the GrFFF fractograms of the total sample (see Fig. 2) from different batches from the same manufacturer. The granule population shows quite a broad, bimodal distribution, as confirmed by the OM pictures taken in correspondence of the two peaks labeled as 1 and 2. The first band corresponds to an average size of 17.1±7.8 μm, while the second corresponds to a value of 6.3±5.6 μm. The retention order in this fractogram is as would be expected from the theory, i.e., the larger particles (fraction 1) are less retained than the smaller ones (fraction 2). The comparison of GrFFF fractograms corresponding to the two batches clearly shows the ability of GrFFF even to screen differences between batches.

It is, therefore, evident that SPLITT is necessary to improve dimensional characterization of such a starch sample and that the chosen SPLITT cut-off (10 μm) is the most suitable choice for preparative, binary fractionation. As previously reported [8], in order to perform a SPLITT separation of samples with a very broad particle size distribution, it is necessary to obtain the parent sample with a cut-off diameter straddling the central portion of the distribution [25]. For this reason a certain amount of the total sample underwent a preliminary gravitational sedimentation to reduce the quantity of large particles (15–50 μm). The cut-off diameter was, thus, set to 15 μm. It must be underlined that, for this kind of sample, when we compute the cut-off diameters we always refer to dry granules and, because of particles swelling, the value may not coincide with that of wet granules.

Fig. 5 shows the GrFFF fractograms of fraction **S2** (the largest granules >15 μm, see Fig. 2), superimposed on the total sample. The maximum of this peak almost coincides with the first peak of the total sample. This means that fraction **S2** contains the largest granules in the total sample (from 28.3 $\mu m_{N=65}$ to 22.2 $\mu m_{N=83}$, as taken from the OM pictures, where N is the number of granules measured by OM) and that the settling has efficiently selected a portion of the population as shown by the absolute absence of peaks in the rest of the fractogram. OM analysis made it possible to convert the

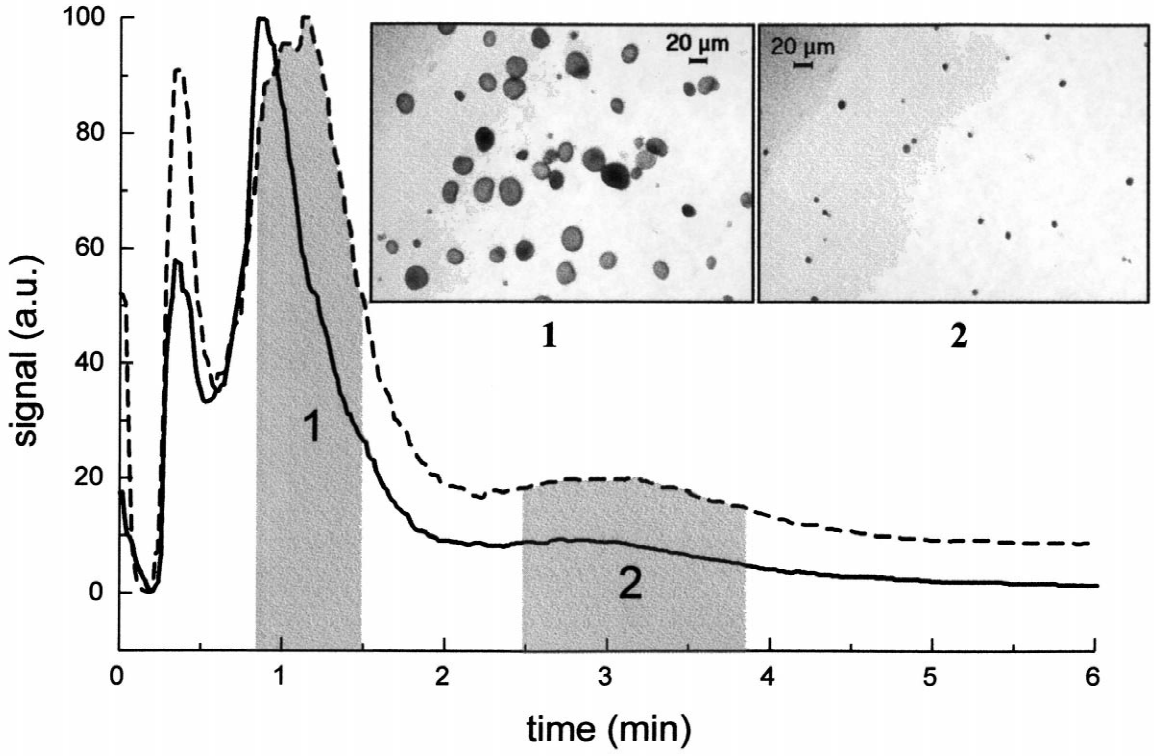

Fig. 4. GrFFF fractograms of two different batches of the wheat total sample. Band areas corresponding to the two collected fractions for OM pictures are shaded.

retention time axis to the diameter scale in Fig. 5 and thereafter. Selectivity was evaluated by the averaged log $V_{r,i}$ of the collected fractions vs. the averaged diameter (as log d_i) [see Eq. (8)] from OM observations. This calibration procedure, based on the observation of granule dimensions, does not implicate a constant density value, but the found linearity in the considered operative range allows the above mentioned conversion. Regression results for the overall data are reported in Table 2. Retention scale was, then, obtained through the use of Eq. (7). In this figure, the almost perfect superimposition of five of the **S2** GrFFF fractograms accumulated for the OM observations, indicated the high reproducibility of the GrFFF procedure. However, this initial separation of the **S2** fraction only serves to halve the quantity of large granules able to interfere with the SPLITT separation. The recovery for this fraction, controlled by the OM was: 90.5% of granules above 15 μm and 9.5% of those smaller than 15 μm.

Fig. 6 compares the fractograms of the total sample to the two final SPLITT fractions **A2** (dotted line) and **B1** (dashed line) respectively containing granules below and above the dry cut-off diameter (10 μm) (see Fig. 2 for the separation scheme). From OM analysis, fraction **A2** and **B1** contained 87% and 10% of the smaller granules (<10 μm), respectively. All the SPLITT runs were adjusted, by applying Eq. (6), to achieve a binary fractionation of 50% around the designated cut-off diameter; that is, where half of the particles exit through outlet **a** and the other half through outlet **b**. Fraction **A2** shows a bimodal distribution, with its secondary maximum recovering the position of the second population of the total sample, i.e., the subpopulation of smallest granules (see band 2, Fig. 4), while fraction **B1** settles below the first peak corresponding to the first population. By comparing Figs. 5 and 6, it is evident that the GrFFF band of the total sample corresponds well to the superimposition of the GrFFF profiles of the two SPLITT fractions **A2** and **B1**, together with the fraction **S2**. This is significant proof of the validity

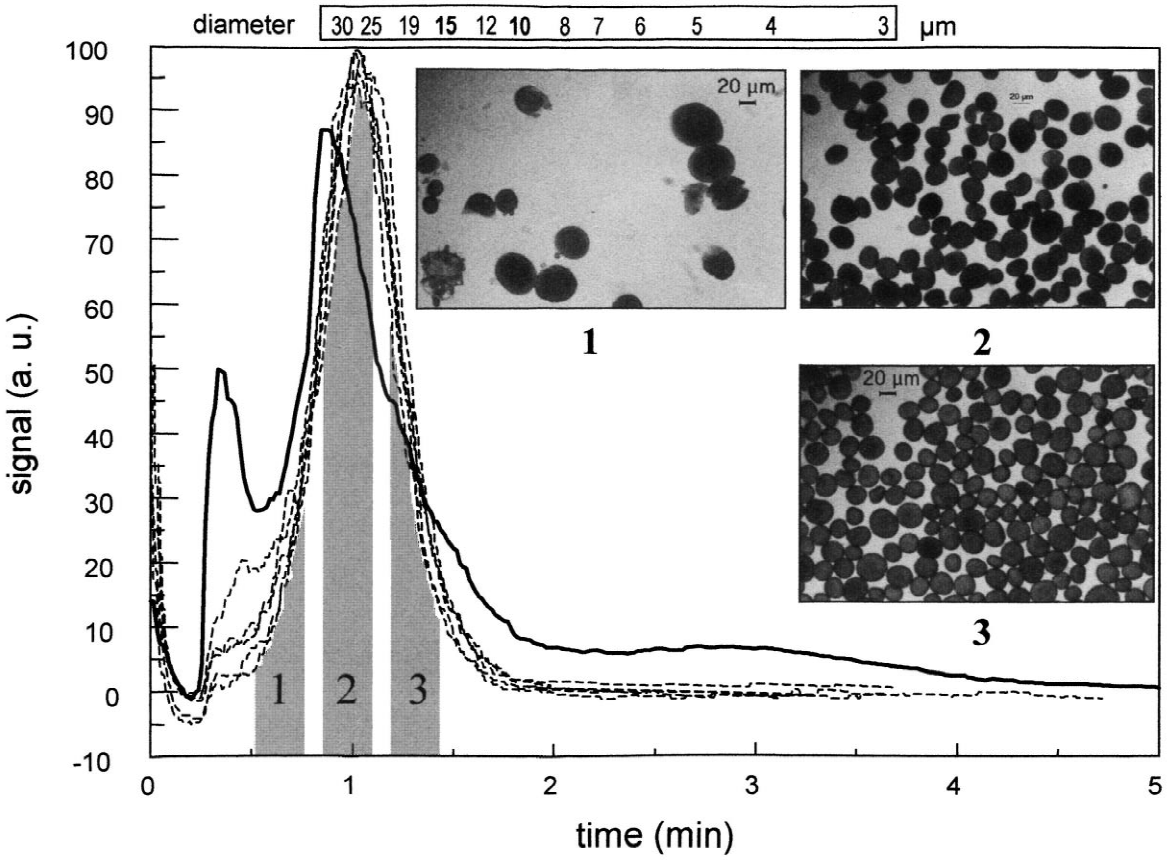

Fig. 5. Repeated GrFFF fractograms of the fraction **S2** (>15 μm) (dashed line), obtained by settling, compared to the GrFFF fractogram of the total sample (full line). Band areas corresponding to the collected fractions for OM pictures are shaded.

of the GrFFF technique in screening SPLITT fractionation results. It also confirms the validity of the GrFFF technique for size characterization.

An evident difference among all these fractograms (Figs. 4–6) is that the void peak appears only when the smallest granules are present as sample or contaminants. In fact, because of the repeated washings, no void peak is present in the fractogram of fraction **S2**. The presence of a significant peak in correspondence to the void can be explained either by lack of an adequate field (Earth's gravity) able to counteract lift forces and focus particles sufficiently close to the accumulation wall to give a certain retention level, or by incomplete sample relaxation during the stop-flow time before GrFFF elution. Both cases may be ascribed to the lower density of the particles eluting with the void vs. the most retained particles, even if the size of the particles correspond. Such density differences could be due to the different swelling of particles with different dry sizes but which could eventually give similar wet sizes. Elution of small granules of similar size actually occurs either as a void peak or in correspondence to the last

Table 2
Evaluation of GrFFF selectivity for the retention-to-size conversion[a]

Fraction	$V_{r,i}$ (cm^3)	Weighted average d_i (μm)	N
A2 (2)	2.75	10.6	174
A2 (3)	5.42	5.7	137
B1 (1)	2.33	17.0	114
S2 (2)	1.92	28.3	65
S2 (3)	2.58	22.2	83

[a] log $V_r = (0.57 \pm 0.19)$ log $d + (1.11 \pm 0.23)$, [see Eq. (7)]; Confidence level: $P = 95\%$; Correlation coefficient: $r = 0.92$.

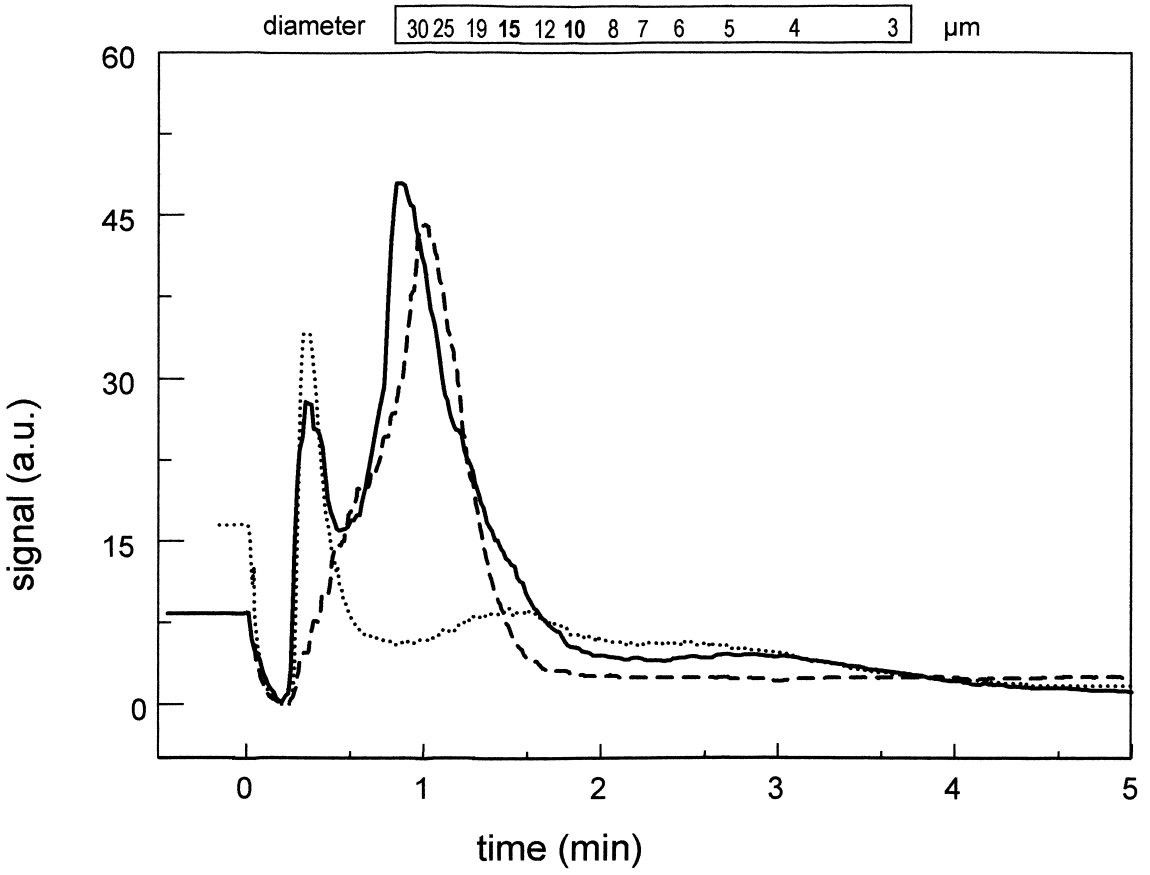

Fig. 6. GrFFF fractograms of the SPLITT fractions **A2** (<10 μm, dotted line) and **B1** (>10 μm, dashed line) compared to the total sample (full line).

band, as shown in the OM pictures of band 1 and 3, fraction **A2** in Fig. 7. From a comparison of the OM pictures it is evident that **A2** particles collected as band 1 and band 3 are indeed quite close in size (band $1=4.63\ \mu m_{N=84}$; band $3=5.04\ \mu m_{N=60}$). However, a full explanation of the effects able to split GrFFF retention of different granule populations of apparently similar size but most likely with different wet densities lies beyond the aim of the present paper.

Fraction **A2** contains a large number of small granules: this finding agrees with the lack of an upper cut-off limit. Fraction **B1** contains small granules only as contaminants, and it is desirable for most of them to be found in fractions **A2** as consequence of the SPLITT treatment. These contaminants, together with physically damaged particles produce the initial shoulder in peak **B1** which is, therefore, broader than expected (Fig. 7).

5. Conclusions

From the above reported study, the complementarity of the two techniques is apparent and their combined use can be promising for many purposes, such as those commonly found in starch studies:

1. GrFFF/PSD to check and control SPLITT separation;
2. Reducing sample complexity by SPLITT separation for the proper GrFFF/PSD characterization of narrowly distributed samples;
3. On line GrFFF–SPLITT coupling in continuous

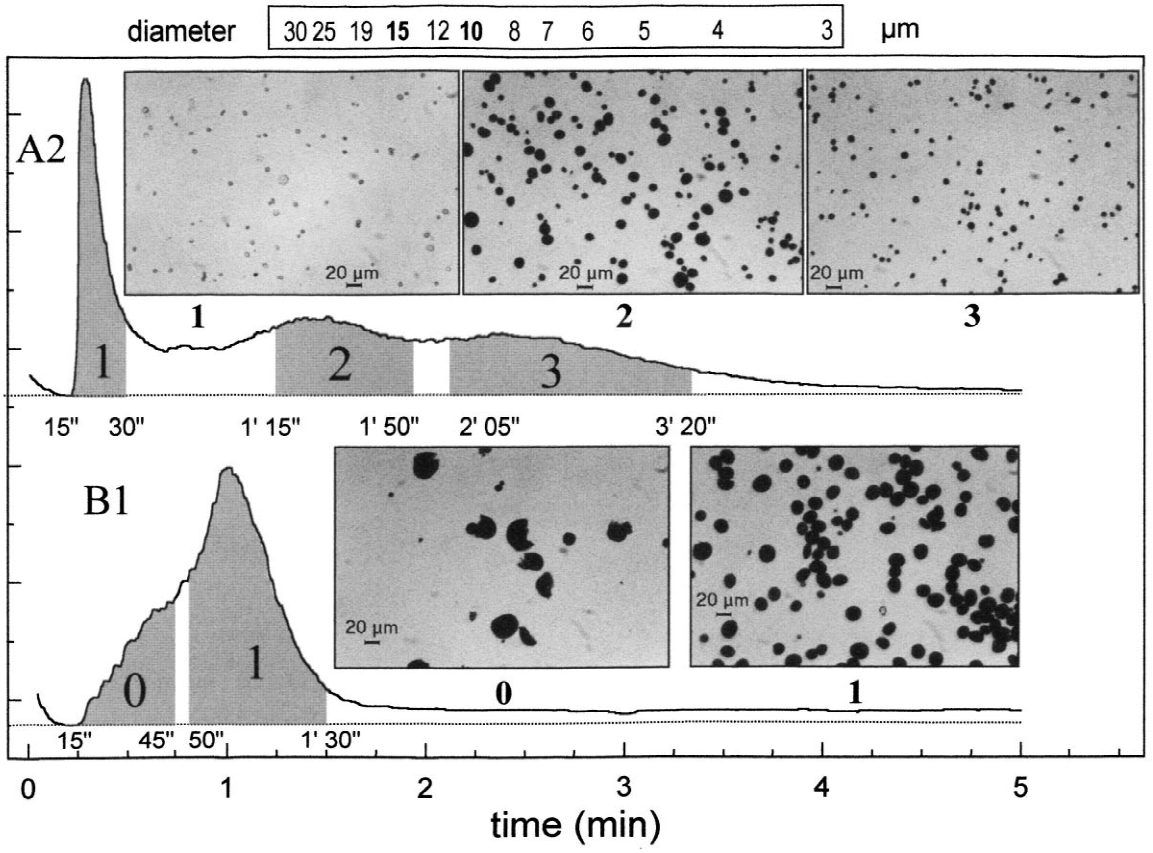

Fig. 7. GrFFF fractograms of the SPLITT fractions **A2** (<10 μm) and **B1** (>10 μm). Band areas corresponding to the collected fractions for OM pictures are shaded.

tuning-monitoring for preparative, binary separation of starches.

Acknowledgements

This work was financially supported by the European Commission Contract No. ERB IC15-CT98-0909, by the Italian Research Council (CNR), by the Italian Ministry of the University and Scientific Technological Research (MURST, 60% and 40%). The authors thank the staff of the Department of Evolutive Biology (University of Ferrara) and of the CNR Center for Macromolecules Studies (Department of Chemistry *G. Ciamician*, University of Bologna) for the use of the optical microscope. Friendly thanks goes to Ferruccio Sembiante for the image processing of the optical microscope pictures.

References

[1] J.L. Jane, in: P.J. Frazier, A.M. Donald, P. Richmond (Eds.), Starch — Structure and Functionality, The Royal Society of Chemistry, 1997, p. 27.
[2] R. Whistler, J.N. BeMiller, E.F. Paschall, Starch — Chemistry and Technology, Academic Press, New York, 1984.
[3] P.S. Williams, S. Levin, T. Lenczycki, J.C. Giddings, Ind. Eng. Chem. Res. 31 (1992) 2172.
[4] S. Levin, G. Tawil, Anal. Chem. 65 (1993) 2254.
[5] C.B. Fuh, M.N. Myers, J.C. Giddings, Anal. Biochem. 64 (1992) 3125.
[6] S.R. Springston, M.N. Myers, J.C. Giddings, Anal. Chem. 59 (1987) 344.

[7] Y. Gao, M.N. Myers, B.N. Barman, J.C. Giddings, Part. Sci. Technol. 9 (1991) 105.
[8] C. Contado, F. Riello, G. Blo, F. Dondi, J. Chromatogr. A 845 (1999) 303.
[9] C. Contado, F. Dondi, R. Beckett, J.C. Giddings, Anal. Chim. Acta 345 (1997) 99.
[10] J.C. Giddings, Science 260 (1993) 1456.
[11] J.C. Giddings, M.H. Moon, P.S. Williams, N.M. Myers, Anal. Chem. 63 (1991) 1366.
[12] M.H. Moon, J.C. Giddings, J. Food Sci. 58 (5) (1993) 1166.
[13] J. Chmelík, A. Krumlova, J. Caslavski, Chem. Pap. 52 (1998) 360.
[14] P. Reschiglian, G. Torsi, Chromatographia 40 (1995) 467.
[15] P. Reschiglian, D. Melucci, A. Zattoni, G. Torsi, J. Microcol. Sep. 9 (1997) 545.
[16] C. Contado, G. Blo, F. Fagioli, F. Dondi, R. Beckett, Colloids Surf. A 120 (1997) 47.
[17] F. Dondi, C. Contado, G. Blo, S. Garçia Martin, Chromatographia 48 (9/10) (1998) 643.
[18] S. Levin, J.C. Giddings, J. Chem. Soc. Tech. Biotechnol. 50 (1991) 43.
[19] S. Gupta, S.P. Lingrani, J.C. Giddings, Sep. Sci Technol. 32 (10) (1997) 1629.
[20] Y. Jiang, A. Kummerow, M. Hansen, J.Microcol. Sep. 9 (1997) 261.
[21] P.S. Williams, T. Koch, J.C. Giddings, Chem. Eng. Commun. 111 (1992) 121.
[22] D. Melucci, G. Gianni, A. Torsi, A. Zattoni, P. Reschiglian, J. Liq. Chromatogr. Rel. Tech. 20 (1997) 2615.
[23] J. Pazourek, K.-G. Wahlund, J. Chmelík, J. Microcol. Sep. 8 (1996) 331.
[24] S.K. Ratanathanawongs, J.C. Giddings, J. Chromatogr. 467 (1989) 341.
[25] Instrument Manual for Series SF1000 SPLITT Particle Separator, Version 1, FFFractionation, Salt Lake City, UT, 1997.